

Topology Exploration in Highly Connected Rare-Earth Metal–Organic Frameworks via Continuous Hindrance Control

Yutong Wang, Liang Feng, Weidong Fan, Kun-Yu Wang, Xia Wang, Xiaokang Wang, Kai Zhang, Xiurong Zhang, Fangna Dai, Daofeng Sun, and Hong-Cai Zhou

J. Am. Chem. Soc., **Just Accepted Manuscript** • Publication Date (Web): 05 Apr 2019

Downloaded from <http://pubs.acs.org> on April 5, 2019

Just Accepted

“Just Accepted” manuscripts have been peer-reviewed and accepted for publication. They are posted online prior to technical editing, formatting for publication and author proofing. The American Chemical Society provides “Just Accepted” as a service to the research community to expedite the dissemination of scientific material as soon as possible after acceptance. “Just Accepted” manuscripts appear in full in PDF format accompanied by an HTML abstract. “Just Accepted” manuscripts have been fully peer reviewed, but should not be considered the official version of record. They are citable by the Digital Object Identifier (DOI®). “Just Accepted” is an optional service offered to authors. Therefore, the “Just Accepted” Web site may not include all articles that will be published in the journal. After a manuscript is technically edited and formatted, it will be removed from the “Just Accepted” Web site and published as an ASAP article. Note that technical editing may introduce minor changes to the manuscript text and/or graphics which could affect content, and all legal disclaimers and ethical guidelines that apply to the journal pertain. ACS cannot be held responsible for errors or consequences arising from the use of information contained in these “Just Accepted” manuscripts.



Topology Exploration in Highly Connected Rare-Earth Metal–Organic Frameworks via Continuous Hindrance Control

Yutong Wang^{†,‡}, Liang Feng^{§,‡}, Weidong Fan[†], Kun-Yu Wang[§], Xia Wang[†], Xiaokang Wang[†], Kai Zhang[†], Xiurong Zhang[†], Fangna Dai[†], Daofeng Sun^{*†}, and Hong-Cai Zhou^{*§#}

[†] School of Materials Science and Engineering, College of Science, China University of Petroleum (East China), Qingdao, Shandong 266580, China

[§] Department of Chemistry, Texas A&M University, College Station, Texas 77843-3255, United States

[#] Department of Materials Science and Engineering, Texas A&M University, College Station, Texas 77843-3003, United States

ABSTRACT: The structural diversity of highly connected metal-organic frameworks (MOFs) has long been limited due to the scarcity of highly connected metal clusters and the corresponding available topology. Herein, we deliberately chose a series of tritopic linkers with multiple substituents to construct a series of highly connected rare-earth (RE) MOFs. The steric hindrance of these substituents can be systematically tuned to generate various linker rotamers with tunable configurations and symmetries. For example, the methyl functionalized linker (L-CH₃) with C_{2v} symmetry exhibits larger steric hindrance, forcing two peripheral phenyl rings perpendicular to the central one. The combination of C_{2v} linkers and 9-connected RE₆ clusters leads to the formation of a new fascinating (3,9)-c **sep** topology. Unlike Zr-MOFs exhibiting Zr₆ clusters in various linker configurations and corresponding different structures, the adaptable RE₆ clusters can undergo metal insertion and rearrange into new RE₉ clusters when connected to an unfunctionalized linker (L-H) with C_1 symmetry, giving rise to a new (3,3,18)-c **ytw** topology. More interestingly, by judiciously combining the linkers with both small and bulky substituents through mixed-linker strategies, a RE₉-based MOF with an engaging (3,3,12)-c **flg** topology could be obtained as a result of continuous steric hindrance control. In this case, the two mixed linkers adopt configurations with moderate steric hindrances. Molecular simulation demonstrates that the combination of substituents with various steric hindrances dictate the resulting MOF structures. This work provides insights into the discovery of unprecedented topologies through systematic and continuous steric tuning, which can further serve as a blueprint for the design and construction of highly complicate porous structures for sophisticated applications.

INTRODUCTION

As a promising class of porous crystalline materials, metal–organic frameworks (MOFs) have attracted growing attention due to their high tunability over their precisely controlled pore environments.^{1–7} The linker length and connectivity, the number and type of functional groups on the linker, the metal node connectivity and nuclearity, and the overall topology can be well manipulated.^{8–10} Among MOFs, highly connected networks have been of a prime interest in recent years, because they reveal underlying principles for the rational design and construction of framework materials.^{11–13} In addition, the resulting structures usually possess outstanding chemical stability, given the fact that harsher conditions are needed to break the higher connectivities in the frameworks during the dissociation process.¹⁰

To enhance the structural diversity of highly connected metal-organic frameworks, several strategies based on the ligand design have been reported.^{9, 14–15} For example, the steric control over ditopic linker based Zr-MOFs have been systematically explored by our group by introducing bulky substituents on the 2- and 2'-positions of BPDC (biphenyl-4,4'-dicarboxylate).^{16–17} The steric hindrance of these substituents

will force the two carboxylates and phenyl rings into a perpendicular configuration, leading to the formation of PCN-700 (PCN = porous coordination network) with a **bcu** net, rather than UiO-67 (UiO = University of Oslo)¹⁸ with a **fcu** net. Speaking of 3-connected linkers, the structural diversity based on highly connected clusters, including Zr₆ or RE₆ (RE = rare earth) can also be expanded by simply tuning steric hindrance and linker configuration. For example, starting from coplanar linkers with D_{3h} symmetry like benzene-1,3,5-tricarboxylate (BTC) or 4,4',4''-s-triazine-2,4,6-triyltribenzoate (TATB), (3,6)-c **spn** topology can form with 6-connected clusters (**Figure 1f**).^{19–21} Similarly, modification of the central phenyl ring of 1,3,5-benzenetribenzoate (BTB) with bulky methyl groups can force the three peripheral phenyl rings perpendicular to the central one, leading to the formation of (3,8)-c **the** topology, although the linker still remains in D_{3h} symmetry.²² In contrast, directly constructing MOFs from 6-connected Zr₆ clusters and BTB³⁻ ligands with C_1 symmetry results in an interpenetrated Zr-BTB MOF.²³ Recently, Yaghi and coworkers reported a **sky** net based (3,12)-c Zr-MOFs based on tritopic linkers with C_s symmetry (**Figure 1a**).²⁴ Additionally, highly connected MOFs based on tetratopic linkers can also be used for advanced topology generation: by tuning the flexible

conformations of ligands, three types of structures with **flu**, **scu**, and **csq** topologies can be obtained from various ligand

rotamers with D_2 , C_{2h} and C_{2v} , respectively.²⁵⁻²⁶ The formation of these (4,8)-connected Zr-tetracarboxylate-based MOFs can

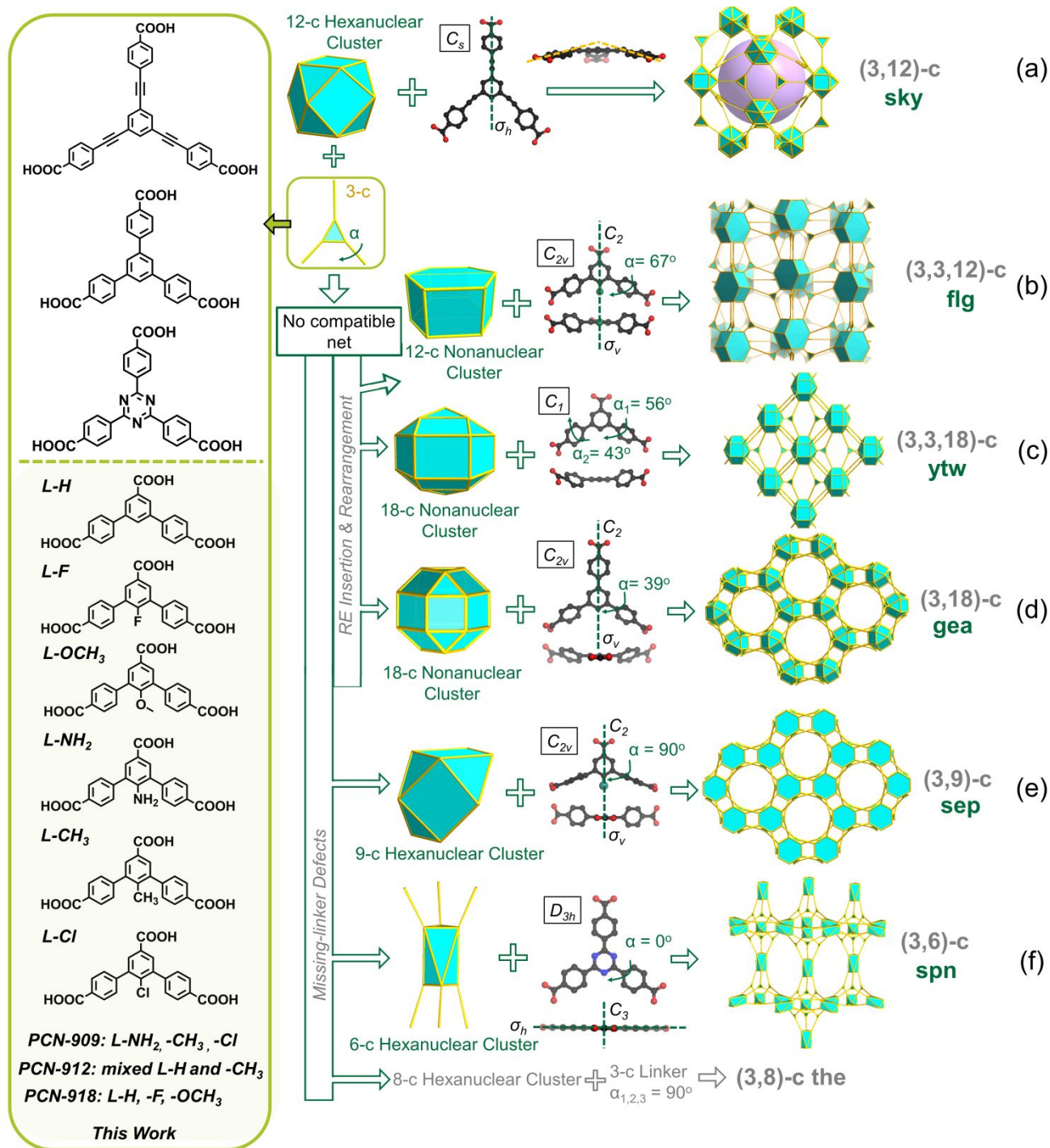


Figure 1. Illustration of various topologies in RE-MOFs based on different linker symmetries: (a) 12-c Zr_6 clusters are linked to tritopic linkers with C_3 symmetry into sky-MOFs; (b) The linking of 12-connected RE_9 clusters with linkers possessing moderate steric hindrance (C_{2v} symmetry) leads to the formation of a flg net; (c) Employment of a C_1 3-c ligand prompted the formation of a novel 18-c RE_9 cluster and its reticulation into a new highly connected (3,3,18)-c ytw net; (d) As expected, use of a C_{2v} 3-c ligand resulted in the discovery of a (3,18)-c gea net reported by Eddaoudi and coworkers; (e) The combination of C_{2v} 3-c ligands and 9-connected RE_6 clusters generates (3,9)-c sep net; (f) The selection of D_{3h} 3-c linkers can induce the formation of (3,6)-c spn net. The inorganic clusters, C, O and N are represented by turquoise, black, red and blue, respectively, and H atoms are omitted for clarity. The linker functional groups and its triangle version in the nets are represented by green.

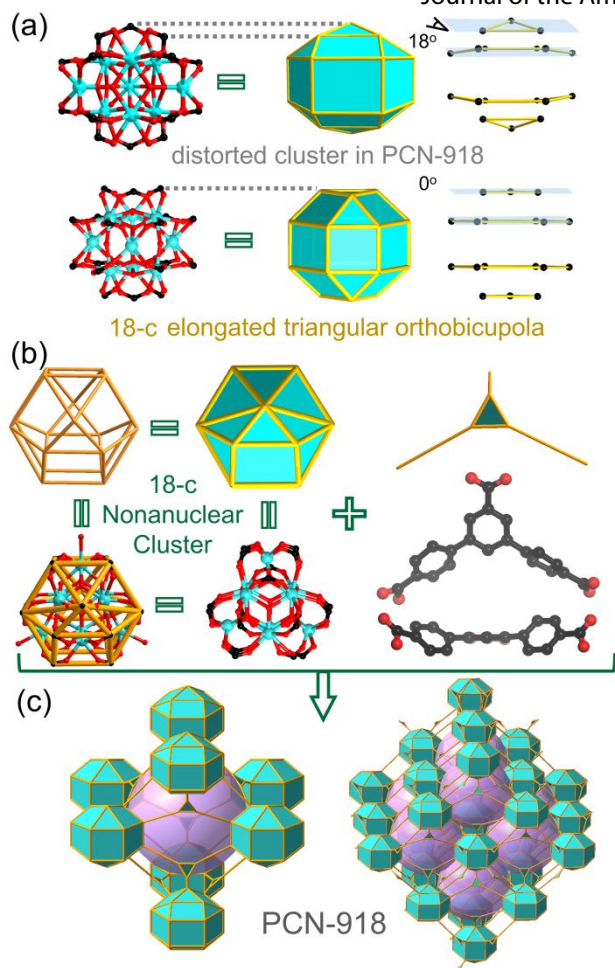


Figure 2. Structural illustration of PCN-918 with (3,3,18)-c ytw topology. (a) The distorted elongated triangular orthobicupola (**eto**) found in PCN-918 with a 18° dihedral angle between the 3-membered and 6-membered rings. For comparison, 18-c RE_9 **eto** clusters found in **gea**-MOF-1 are presented with all four rings parallel. (b) The assembly of 18-c RE_9 clusters and 3-c ligands with bulky substituents (C_1) into a (3,3,18)-c **ytw** net. (c) Illustration of cluster packing and pore arrangement in PCN-918.

be systematically tuned by altering the substituent positions on linkers. So far, the steric control over linker configuration in Zr-MOFs has been proven as a successful strategy because of their predictable and well-maintained Zr_6 clusters. However, this structural uniformity also poses a challenge to the discovery of new and intricate topologies especially in highly connected networks for sophisticated applications.²⁷ Therefore, it is important to find highly connected MOFs with relatively labile and dynamic substituents for previously reported Zr_6 clusters, which can still be selectively bonded to linkers with controllable configurations and symmetries.

RE based clusters are suitable candidates for the design and construction of intricate topologies because the RE hard-sphere behavior allows for multiple directionality of coordinated ligands.²⁸⁻³⁰ Typically, each RE cation can coordinate with six to twelve terminal ligands while each Zr cation can only coordinate with eight. Moreover, the moderate RE-O bond strength, along with the higher ion coordination numbers, gives

rise to a large library of novel and intricate polynuclear clusters, leading to the formation of sophisticated frameworks and their corresponding topologies.^{11-13, 21, 29, 31-34} For instance, Eddaoudi and coworkers reported a series of hexanuclear RE_6 clusters-based frameworks through reticular chemistry design.¹¹⁻¹² When linked to tritopic linkers that exhibited no compatible network, this hexanuclear RE_6 cluster tended to undergo rearrangements and form nonanuclear RE_9 clusters that present distinct coordination behaviors. For example, **gea**-MOF-1, with a (3,18)-connected net, can be constructed from the 18-connected RE_9 clusters and BTB ligands (**Figure 1d**), while **aea**-MOF-1 and **pek**-MOF-1 can be built from 12-connected RE_9 clusters and 3-connected organic ligands with lower symmetry.^{13, 32} In addition, mixed-linker or multivariate (MTV) strategies have recently been employed in RE-MOFs to amplify their structural diversity and function integrity.^{21, 31} However, it still remains challenging to uncover elaborate and unprecedented topologies, or control the formation of highly connected MOFs through rational design.

Herein, we deliberately chose a series of tritopic linkers with multiple substituents to construct highly connected rare-earth (RE) MOFs. The steric hindrance of these substituents can be systematically tuned to generate various linker rotamers with tunable configuration and symmetries. For example, the methyl functionalized linker (L- CH_3) with C_{2v} symmetry exhibits larger steric hindrance, forcing two peripheral phenyl rings perpendicular to the central one. The combination of C_{2v} linkers and 9-connected RE_6 clusters leads to the formation of a new fascinating (3,9)-c **sep** topology (**Figure 1e**). Unlike Zr-MOFs exhibiting preserved Zr_6 clusters in numerous structures with various linker configurations, RE_6 clusters can undergo metal insertion and rearrange into new RE_9 clusters when connected to the nonfunctionalized linker (L-H) with C_1 symmetry, giving rise to a new (3,3,18)-c **ytw** topology (**Figure 1c**). More interestingly, by judiciously combining the linkers with both bulky and low steric substituents through mixed-linker strategies, a RE_9 -based MOF with an engaging (3,3,12)-c **flg** topology was obtained as a result of continuous steric hindrance control (**Figure 1b**). In this case, two mixed linkers adopt configurations with moderate steric hindrances. The abovementioned torsion angles between the central phenyl ring and the peripheral ring can be well tuned, while the torsion angles between the peripheral phenyl ring and the coordinating carboxylate groups are negligible, less than 10° in all cases. Molecular simulations demonstrate that the combination of substituents with various steric hindrances dictates the resulting MOF structures. This work provides insights into the discovery of unprecedented topologies through systematic and continuous steric tuning, which can further serve as blueprints for the design and construction of highly complicate porous structures for sophisticated applications.

RESULTS AND DISCUSSION

Design, Synthesis and Structural Description. Herein we selected six tritopic ligands with various substituents (-H, -F, -OCH₃, -NH₂, -CH₃, -Cl) to construct RE-MOFs that exhibit multiple unprecedented topologies. As shown in **Figure 1**, the functional groups with various levels of steric hindrance are introduced at the -R position, tuning the rotation of two peripheral phenyl rings near the central one.

Solvothermal reactions between L-Cl, -CH₃ or -NH₂ and Eu(NO₃)₃·6H₂O in the presence of 2-fluorobenzoic acid (2-FBA) for 24 h yielded large colorless crystals with hexagonal prism morphology, PCN-909 (also named UPC-909). With 2-FBA as a modulator, hexanuclear RE clusters can easily form *in situ* and further be utilized for the construction of extended frameworks.¹³ The formula of PCN-909 was determined by single-crystal X-ray diffraction. In contrast, under the same condition, the reaction between Eu(NO₃)₃·6H₂O and L-H, -F, or -OCH₃ yields large cuboid crystals with a new *ytw* net, donated as PCN-918 (also named UPC-918). The powder X-ray diffraction (PXRD) patterns also indicate the phase purity of the aforementioned products. Notably, PCN-909-NH₂ formed by L-NH₂ was often obtained in accompaniment with another crystalline cuboid phase, donated as PCN-912 (also named UPC-912).

Interestingly, these results indicate that when linkers with low steric hindrance, for example H, F and OCH₃, are used to construct extended frameworks, PCN-918 is always obtained as a pure phase, named as PCN-918-H, -F and -OCH₃, respectively. L-H, with only -H as a substituent at the -R position tends to adopt a C₇ symmetry in the frameworks due to asymmetric rotation of C-C bonds between the two peripheral phenyl rings and the central one. Substituting H with F or OCH₃, substituents with similar steric properties, has negligible effects on the dihedral angle change between the two peripheral phenyl rings.

PCN-918 represents a rare MOF composed of metal clusters with a high connectivity number (18-connected). PCN-918 crystallized in the orthorhombic space group *Pmmn* (Table S1). Crystallographically, it contains an 18-connected RE₉ cluster [RE₉(μ₃-OH)₈(μ₂-OH)₃(O₂C-) ₁₈] and a tritopic linker with C₇ symmetry. Each RE₉ cluster is connected by eighteen adjacent L-R linkers, which can be simplified into a 3,3,18-connected net with *ytw* topology (Figure 2). Topologically, the 18-connected metal clusters can be regarded as distorted elongated triangular orthobicupola (*eto*) nodes and tritopic linkers can be

viewed as triangular nodes (Figure 2b). The overall structure was analyzed to be a 3,3,18-connected net with a point symbol of {4³}₆{4⁴².6⁷².8³⁹} as determined by TOPOS 4.0 (Figure 2c)³⁵.

For clarity, the cluster structure of PCN-918 was described and compared with its analogous cluster found in *gea*-MOF-1. In *gea*-MOF-1, the RE₉ cluster is capped by 18 carboxylates arranged in an elongated triangular orthobicupola manner. As shown in Figure 2a, the 18 carboxylates consist of two 3-membered rings at the top and bottom sides and two 6-membered rings in the middle. These rings are parallel to each other in *gea*-MOF-1. However, in PCN-918, the 18 carboxylates are linked in a more distorted way, leading to an 18° dihedral angle between the 3-membered and 6-membered rings.

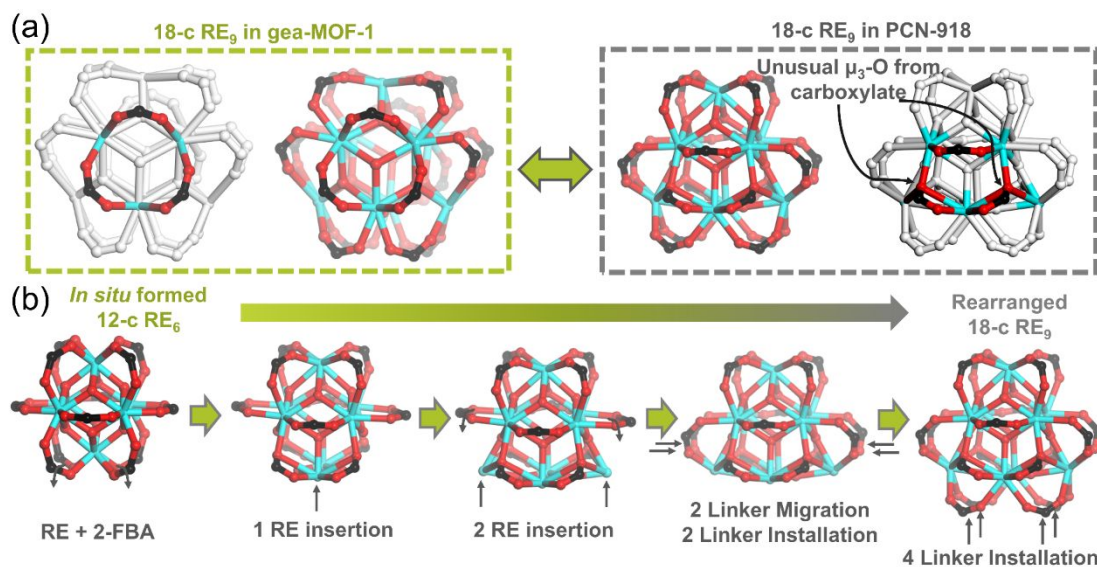


Figure 3. Proposed pathway for the evolution from 12-connected RE₆ clusters to 18-connected RE₉ clusters. (a) Comparison of 18-c RE₉ in *gea*-MOF-1 and PCN-918. In PCN-918, oxygens from two out of three highlighted carboxylates coordinate with three RE cations, acting as a bridging oxygen. (b) Proposed metalation, linker migration, and installation process during the rearrangement of RE clusters.

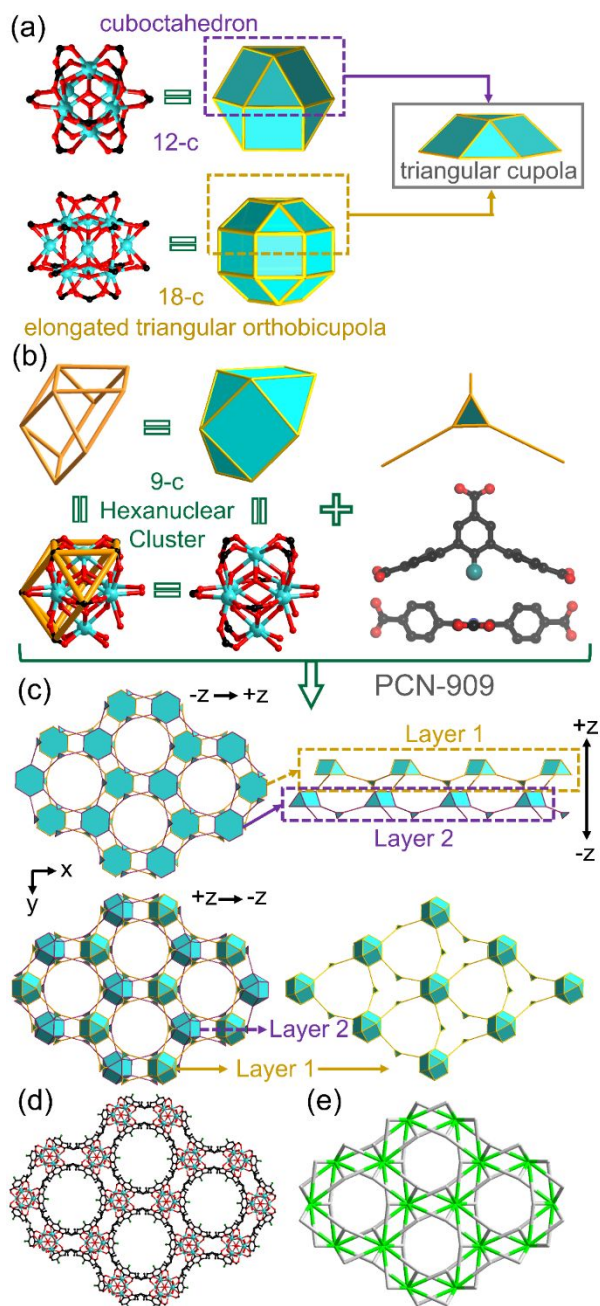


Figure 4. Structural illustration of PCN-909 with (3,9)-c sep topology. (a) The triangular cupola, representing 9-connected RE_6 clusters, can be viewed as half a cuboctahedron or a part of an elongated triangular orthobicupola (**eto**); (b) The assembly of 9-c RE_6 clusters and 3-c ligands with bulky substituents (C_{2v}) into a (3,9)-c **sep** net. (c-e) The hexagonal close packing of the 9-c RE_6 clusters of PCN-909 was observed with all triangular cupola clusters placed in same direction. Layers 1 and 2 from the hexagonal packing are represented in yellow and purple, respectively.

This distorted dihedral angle in the RE_9 clusters of PCN-918 originates from the nonidentical coordination environments for the carboxylates forming 3-membered rings. In **gea**-MOF-1, each oxygen from these carboxylates coordinates with one RE cation. However, in PCN-918, only one carboxylate out of these acts in this manner, while the oxygen in the other two carboxylates tends to coordinate with three RE cations, with one oxygen atom acting as a bridging oxygen (**Figure 3**). This coordination behavior is quite similar to what we have observed previously in the case of cluster metalation, where cooperative cluster metalation and ligand migration in Zr-MOFs have been captured through single-crystal X-ray diffraction.³⁶ This led us to propose a complementary path explaining the evolution from the RE_6 cluster to the RE_9 cluster. The *in situ* formed RE_6 clusters from the 2-FBA modulated synthesis have been well documented in literatures.¹³ Due to the adaptable nature of the RE clusters, insertion of three RE cations around the RE_6 clusters without decomposing the clusters can be easily achieved. The insertion of more exposed RE sites is believed to induce the linker migration and installation, leading to the formation of the rearranged 18-connected RE_9 clusters.¹⁶

Modification of central phenyl ring of L-H with bulky methyl or chloride groups can force two peripheral phenyl rings perpendicular to the central one, leading to the formation of PCN-909. Single-crystal X-ray analysis revealed that PCN-909 crystallized in the hexagonal space group $P6_3mc$ (**Figure 4**). It contains a 9-connected RE_6 cluster [$RE_6(OH)_8(O_2C^-)_9$] and a tritopic linker with C_{2v} symmetry. Crystallographically, nine tritopic linkers bridged three neighboring RE_6 clusters, which can be simplified into a 3,9-connected net with **sep** topology (**Figure 4c**). Topologically, the 9-connected metal clusters can be regarded as triangular cupola nodes and the tritopic linkers can be viewed as triangular nodes (**Figure 4a-b**). The triangular cupola, representing 9-connected RE_6 clusters, can be viewed as half a cuboctahedron (12-connected RE_6 clusters) and part of an elongated triangular orthobicupola (**eto**, 18-connected RE_9 clusters). The overall structure was analyzed to be a 3,9-connected net with a point symbol of $\{4^2.6\}_3\{4^6.6^2.8^6\}$ as determined by TOPOS 4.0 (**Figure 4c-e**).

The PCN-909 framework here represents the high adaptability of RE polynuclear clusters; when the linker configuration is altered, local missing-linker defects might be found on the corresponding RE cluster, allowing for the formation of an extended ordered framework. The points of extension (n-connectivity) in the parent 12-c RE_6 clusters formed in the presence of 2-FBA is reduced to nine, with this being the first known example of this process in RE-MOFs, to the best of our knowledge. Particularly, in the 12-c RE_6 cluster, three of the twelve carboxylate moieties, originally linking as points of extension in MOFs with **fcu** topology, are replaced by terminal carboxylates (2-FBA or formate anions from the DMF decomposition). These terminal ligands can be further replaced by soaking in water, allowing for the remaining nine connecting carboxylates to arrange in a triangular cupola manner.

Interestingly, PCN-909 has a similar topological structure as observed in **gea**-MOF-1, although the connectivity and configuration of clusters in both MOFs are quite different from each other. Hexagonal close packing of the 9-c RE_6 clusters of PCN-909 was observed in a manner similar to the packing of the 18-c RE_9 clusters in **gea**-MOF-1. As indicated in **Figure 4c**,

all 9-c RE₆ clusters, simplified as triangular cupola units, are arranged in same direction. The staggered arrangement of clusters in two layers are linked by the tritopic linkers with C_{2v} symmetry. Note that the linkers in **gea**-MOF-1 also exhibit C_{2v} symmetry, but with a lower dihedral angle between the central phenyl ring and the two peripheral ones.

Topology Exploration by Multivariate Strategy. The preliminary results here enable us to tune the formation of various phases with unprecedented topologies by simply controlling the steric effects of linkers. However, RE-MOFs constructed from single linkers with a simple variation of functional groups can only achieve a few discrete energy states caused by steric exclusion effects. Alternatively, a mixed-linker, or so-called multivariate (MTV) strategy, allows for the continuous creation of energy states associated with tunable steric hindrances.³⁷⁻³⁸

In the case of Zr-based PCN-605, 606 and 608 series, where the Zr₆ clusters are stable enough to preserve the configuration without undergoing rearrangement; by doping a small amount of linker with a more free configuration into a more restricted conformation.²⁶ However, in the case of RE-based MOFs, the RE cluster is more labile and prone to undergo rearrangement to access frameworks with minimized energy based on the formation of the RE-carboxylate bond being an exothermic process. We expect that by mixing linkers with both more and less sterically hindered substituents in a controllable manner we can achieve a continuous tunability of the steric hindrances of the overall system, which might further lead to the discovery of unique structures and topologies. Various ratios of the less hindered L-H were then incorporated into mixtures with the other five linkers with different functional groups (-F, -OCH₃, -NH₂, -CH₃ and -Cl, respectively) during solvothermal reactions. Remarkably, by doping a certain amount of linker (L-H, C₁ symmetry) with low steric hindrance with a bulky linker (L-CH₃, C_{2v} symmetry with 90° dihedral angle), it will force both linkers into a less favorable state (L-H and -CH₃, C_{2v} symmetry with 67° dihedral angle), associated with the rearrangement of the RE clusters and the formation of the PCN-912 framework.

The pure single-crystalline cuboid phase of PCN-912 was formed with a moderate connectivity number (12), as compared to the parent PCN-909 with a low connectivity number (9) and PCN-918 with a high connectivity number (18). Single-crystal X-ray analysis revealed that PCN-912 crystallizes in the tetragonal space group *I4₁/acd*. PCN-912 contains a 12-connected RE₉ cluster [RE₉(μ₃-OH)₁₂(μ₃-O)₂(O₂C⁻)₁₂] and a tritopic linker with C_{2v} symmetry. Crystallographically, the 12-connected metal clusters can be regarded as hexagonal prism nodes and the tritopic linkers can be viewed as triangular nodes (**Figure 6**). The overall structure was analyzed to be a 3,3,12-connected net with a point symbol of {4¹⁸.6³⁰.8¹⁸} {4².6²}₂ {4³}₂ as determined by TOPOS 4.0 (**Figure 6b-c**).³⁵

The 12-connected nonanuclear RE₉ cluster, reported

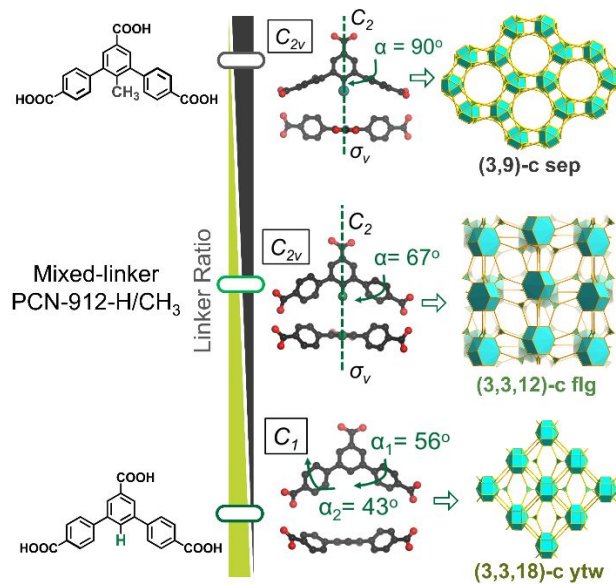


Figure 5. Continuous tuning of linker steric hindrance through multivariate (MTV) strategy. By mixing a certain amount of linker (L-H, C₁ symmetry) with low steric hindrance into a bulky linker (L-CH₃, C_{2v} symmetry with 90° dihedral angle), it will force both linkers into a less stable state (L-H and -CH₃, C_{2v} symmetry with 67° dihedral angle), associated with the rearrangement of RE clusters and formation of PCN-912.

previously by Eddaoudi and coworkers, is linked by 12 carboxylates arranged in a hexagonal prism way.³² The points of extension in the parent 18-c RE₉ clusters is reduced to twelve, with the three carboxylate moieties missing on the top and bottom side of the RE₉ clusters, respectively (**Figure 6a**). In the structure of PCN-912, each two neighboring RE₉ clusters are perpendicular to each other due to the rotation of the RE₉ clusters caused by the length variation of the tritopic linkers (**Figure 6c**). Noticeably, both of the linkers are forced into a confined state with 67° dihedral angle between the central phenyl ring and the two peripheral ones. The ratio of L-CH₃ and L-H found in the mixed-linker PCN-912(Eu)-CH₃ was calculated from the ¹H NMR of digested MOF samples (**Table S6**). As indicated from the ¹H NMR results, the ratio of L-H found in the structure of final product PCN-912(Eu)-CH₃ increases as the ratio of L-H in the precursor increases.

A phase diagram summarizing this multivariate strategy is shown **Figure S25**, illustrating the power of multivariate strategy to functionalize targeted frameworks, limiting the growth of the impure phase during the solvothermal reactions and allowing for the discovery of unprecedented structures. For instance, the synthesis of the single-linker PCN-909-NH₂ always contains a small amount of PCN-912-NH₂ impurity as indicated by PXRD patterns; by mixing L-NH₂ and L-H, MTV-PCN-918-NH₂ can be obtained without impurities.

To further verify the versatility of topology exploration in RE-MOFs via continuous hindrance control, PCN-9XX(RE, XX = 09, 12 and 18) analogues with various RE metals (i.e., Eu, Y, Ce, Yb, Tb, Dy) have also been successfully synthesized under similar reaction conditions, as indicated by PXRD patterns (**Figure S11-13**).

Formation Mechanism of Multiple Topologies. Unlike Zr-MOFs exhibiting preserved Zr₆ clusters in numerous structures with various linker configurations, RE₆ clusters are more adaptable, with the cluster form being dependent on the linker configuration. Our work suggests that when highly connected polynuclear RE clusters are linked to various linkers, crystalline extended structures with preserved cluster configurations and connectivities are formed initially. However, in order to reach topologies that result in low energy structures, these RE cluster can undergo three types of alterations: a) the reduction of points of extension (n-connectivity) in the parent clusters, b) the preservation or c) increase of points of extension in the parent clusters by cluster metalation and rearrangement. By systematically modifying the central phenyl ring on L-H, bulky groups can force the rotation of the two peripheral phenyl rings, leading to various unprecedented topologies.

The effects of ligand hinderance on steric control have been investigated through density functional theory (DFT) calculations. The energies of selected linkers in PCN-909, PCN-912, and PCN-918 are calculated and summarized in **Figure 7**. For clarity, all energies are normalized through subtracting the energy of the unconstrained structure of a given ligand. Owing to the constraints from RE₆ or RE₉ clusters in confined frameworks, ligands in the three phases with different topologies demonstrate distinct torsion angles between the peripheral and central phenyl rings. By comparing the relative energies of linkers in PCN-909 and PCN-918, ligands with bulky groups such as -CH₃, -Cl, and -NH₂ tend to be obtained with a larger torsion angle, while for ligands modified with groups such as -H, -F and -OCH₃, a smaller torsion angle is favored, which confirms the point that steric bulk in a ligand is beneficial for the formation of PCN-909.

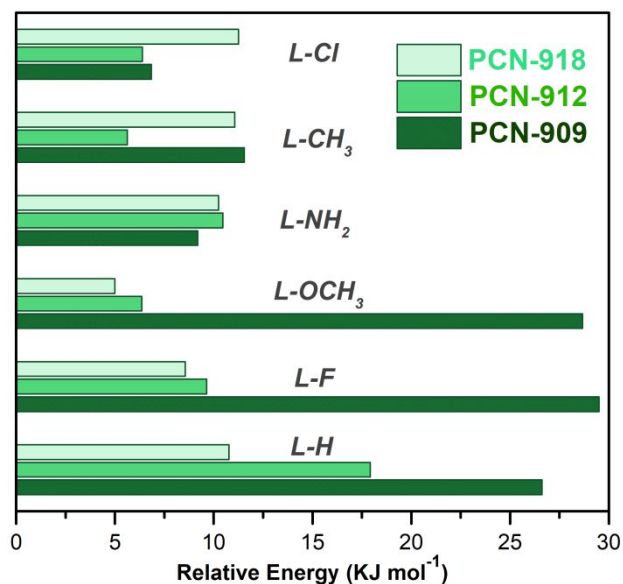


Figure 7. Relative energies of ligands with various configurations in PCN-9XX series possessing different topologies. The relative energy for a given ligand is normalized through subtracting the energy of its unconstrained structure.

The energy difference of L-CH₃ in PCN-912 and PCN-909 is ~5.9 kJ/mol, while the difference is ~7.1 kJ/mol for L-H in

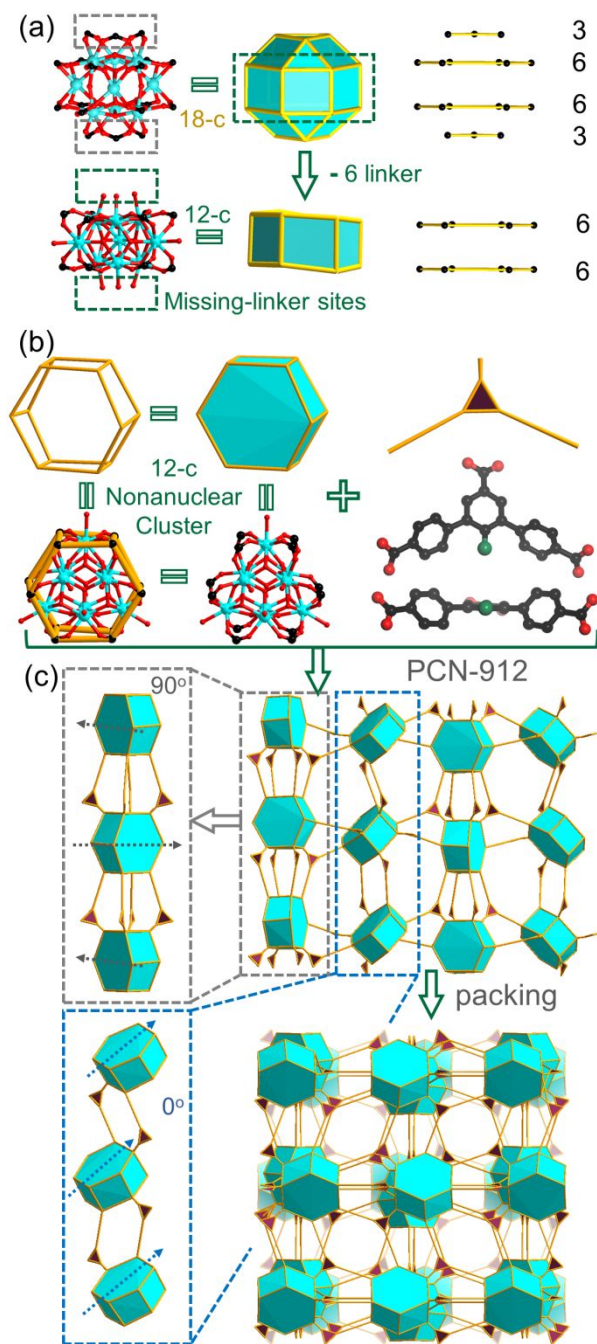


Figure 6. Structural illustration of PCN-912 with (3,3,12)-c topology. (a) The hexagonal prism, representing 12-connected RE₉ clusters, can be viewed as a part of an elongated triangular orthobicupola (**eto**) by removing six linkers on the top and bottom side of a 18-connected RE₉ clusters. (b) The assembly of 12-c RE₉ clusters and mixed 3-c ligands (C_{2v}) into a (3,3,12)-c **flg** net. (c) Illustration of cluster packing and pore arrangement in PCN-912.

PCN-912 and PCN-918. This result indicates that the formation of PCN-912 only needs to cross a relative low energy barrier, from a linker perspective. Yet, calculation on the relative

energies of the ligands is only one perspective needed to understand how ligand sterics controls the topologies of RE-MOFs. Other factors such as solvent molecules, metal node nuclearity and connectivity should also contribute to the variation on RE-MOF topologies.

Stability, Porosity and Gas Sorption Studies. The thermal stability of PCN-909, PCN-912 and PCN-918 were determined by thermogravimetric analysis (TGA, **Figure S57-63**). The initial weight loss before 120 °C is attributed to the removal of the solvent molecules in the pores, whereas the weight loss from 200 to 300 °C can be attributed to the removal of strongly coordinated DMF or DMA cations trapped inside the pores. The decomposition of PCN-909, 912 or 918 starts at 550 °C, leading to the removal of organic linkers and structural collapse. In addition, the chemical stability of PCN-9XX(RE) was examined by soaking the MOFs in various solvents for 24 h. PXRD patterns suggest that the PCN-912 and PCN-918 have excellent stability due to the retained crystallinity in most solvents, including DMF, acetone, CH₃OH, EtOH, CH₃CN, and water (**Figure S17-19**). PCN-909 with much lower connectivity number demonstrate good stability only in organic solvents, however, it will gradually get decomposed when exposed to water (**Figure S6-8**). The presence of various functional groups was also supported by infrared (IR) spectroscopy (**Figure S26-28**).

The permanent porosity of the PCN-9XX(RE, XX = 09, 12 and 18) series was confirmed by N₂ adsorption isotherms measured at 77 K (**Figure S29-34**). Prior to the gas sorption measurements, PCN-9XX series samples were rinsed thoroughly using DMF and fresh acetone for three days before thermal activation at 100°C under vacuum. PCN-918(Eu) exhibits a saturated uptake of 216 cm³ g⁻¹ at 1 atm, with the other PCN-9XX(Eu) series also showing similar N₂ adsorption isotherms, with slightly lower surface areas due to the presence of bulkier substituents.

Due to the intrinsic permanent porosity and channel environments of PCN-9XX(RE), their potential application for light hydrocarbon (CH₄, C₂H₂, C₂H₄, C₂H₆, C₃H₆, and C₃H₈) adsorption (**Figure S35-48**) and separation (**Figure S49-56**) has been investigated systematically. It was found that PCN-909(Tb)-NH₂ shown a much higher heats of adsorption for C₃ light hydrocarbons, indicating stronger affinities for these gases to be adsorbed on the framework. We further conducted ideal solution adsorbed theory (IAST) for binary equimolar components to study the potential for the separation of CH₄ from C₃ light hydrocarbons.³² At 1 bar and 298 K, the selectivities for C₃H₈ and C₃H₆ over CH₄ are 96.9 and 97.6 respectively, making PCN-909(Tb)-NH₂ a promising adsorbent for the efficient removal of C₃ light hydrocarbons from natural gas streams at room temperature.

CONCLUSIONS

In conclusion, we report a highly tunable RE-MOF system that contains a series of tritopic linkers with multiple substituents. Depending on the sizes of these substituents, the linkers can generate various rotamers with tunable configurations and symmetries that have resulted in the discovery of three unprecedented and fascinating topologies. The combination of methyl functionalized linker (L-CH₃) with C_{2v} symmetry and the 9-connected RE₆ clusters led to the

formation of a (3,9)-c **sep** topology, while the linked RE₉ clusters with a nonfunctionalized linker (L-H) with C₇ symmetry, gave rise to a new (3,3,18)-c **ytw** topology. More interestingly, continuous steric hindrance control can be achieved by judiciously combining the linkers with both bulky and compact substituents, leading to the formation of a RE₉-based MOF with an engaging (3,3,12)-c **flg** topology. This work indicates that highly complicate networks can be rationally designed and constructed through systematic and continuous steric tuning, which will bring insights into the design and construction of tailored porous frameworks for sophisticated applications.

EXPERIMENTAL SECTION

Materials and Instrumentation. All reagents and solvents used in the synthetic studies were commercially available and used as supplied without further purification. The ligands were synthesized through the procedures in Supporting Information Section 1. ¹H NMR spectra were obtained on an Inova 500 MHz spectrometer. Single crystal X-ray diffraction experiments were carried out on a SuperNova diffractometer equipped with mirror Cu-K α radiation ($\lambda = 1.54184 \text{ \AA}$) and an Eos CCD detector under 150 K. Powder X-ray diffraction (PXRD) was carried out with a Bruker D8-Focus Bragg-Brentano X-ray Powder Diffractometer equipped with a Cu sealed tube ($\lambda = 1.54178 \text{ \AA}$) at 40 kV and 40 mA. Gas sorption measurements were conducted on a Micromeritics ASAP 2020 system. PCN-909, 912 and 918 (or UPC-909, 912 and 918) are named based on the cluster connectivity.

Synthesis of PCN-918(Eu). Eu(NO₃)₃ (15 mg), H₃L (10 mg) and 1 mol/L 2-fluorobenzoic acid DMF solution (3 mL) were charged into a 10 mL vial. The mixture was heated in 115 °C oven for 2 days. After cooling down to room temperature, the colorless crystals of PCN-918(Eu) were harvested (yield: 66%).

Synthesis of PCN-918(Eu)-F. Eu(NO₃)₃ (15 mg), H₃L-F (10 mg) and 1 mol/L 2-fluorobenzoic acid DMF solution (3 mL) were charged into a 10 mL vial. The mixture was heated in 115 °C oven for 2 days. After cooling down to room temperature, the colorless crystals of PCN-918(Eu)-F were harvested (yield: 65%).

Synthesis of PCN-918(Eu)-OCH₃. Eu(NO₃)₃ (15 mg), H₃L-OCH₃ (10 mg) and 1 mol/L 2-fluorobenzoic acid DMF solution (3 mL) were charged into a 10 mL vial. The mixture was heated in 115 °C oven for 2 days. After cooling down to room temperature, the colorless crystals of PCN-918(Eu)-OCH₃ were harvested (yield: 65%).

Synthesis of PCN-909(Eu)-NH₂. Eu(NO₃)₃ (15 mg), H₃L-NH₂ (10 mg) and 1 mol/L 2-fluorobenzoic acid DMF solution (3 mL) were charged into a 10 mL vial. The mixture was heated in 115 °C oven for 2 days. After cooling down to room temperature, the colorless crystals of PCN-909(Eu)-NH₂ were harvested (yield: 64%).

Synthesis of PCN-909(Eu)-CH₃. Eu(NO₃)₃ (15 mg), H₃L-CH₃ (10 mg) and 1 mol/L 2-fluorobenzoic acid DMF solution (3 mL) were charged into a 10 mL vial. The mixture was heated in 115 °C oven for 2 days. After cooling down to room temperature, the colorless crystals of PCN-909(Eu)-CH₃ were harvested (yield: 67%).

Synthesis of PCN-909(Eu)-Cl. Eu(NO₃)₃ (15 mg), H₃L-Cl (10 mg) and 1 mol/L 2-fluorobenzoic acid DMF solution (3 mL) were charged into a 10 mL vial. The mixture was heated in 115 °C oven for 2 days. After cooling down to room temperature, the colorless crystals of PCN-909(Eu)-Cl were harvested (yield: 66%).

Synthesis of PCN-912(Eu)-P%CH₃ (P = 35%, 50% and 65%). Eu(NO₃)₃ (15 mg), H₃L-CH₃ (3.5, 5, and 6.5 mg, respectively), H₃L (6.5, 5, and 3.5 mg, respectively), and 1 mol/L 2-fluorobenzoic acid DMF solution (3 mL) were charged into a 10 mL vial. The mixture was heated in 115 °C oven for 2 days. After cooling down to room temperature, the colorless crystals of PCN-912(Eu)-P%CH₃ were harvested.

Synthesis of MTV-PCN-9XX(Eu)-P%L-R (XX = 09, 12 and 18). Eu(NO₃)₃ (15 mg), H₃L-R (p mg), H₃L (10-p mg), and 1 mol/L 2-fluorobenzoic acid DMF solution (3 mL) were charged into a 10 mL vial. The mixture was heated in 115 °C oven for 2 days. After cooling down to room temperature, crystals of MTV-PCN-9XX(Eu)-P%L-R were harvested.

ASSOCIATED CONTENT

Supporting Information. The Supporting Information is available free of charge on the ACS Publications website at DOI:10.1021/jacs.xxxxxx.

Text, tables, and figures giving experimental procedures for the syntheses of the ligands, PXRD, gas adsorption isotherms, ¹H NMR spectra, and other additional information (PDF)

X-ray crystallographic details of the structures (CIF)

AUTHOR INFORMATION

† Y. T. Wang and L. Feng contributed equally to this work.

Corresponding Author

*dfsun@upc.edu.cn

*zhou@chem.tamu.edu

Notes

The authors declare no competing financial interest.

ACKNOWLEDGMENT

This work was financially supported by the National Natural Science Foundation of China (NSFC Grant Nos. 21875285, 21571187), Taishan Scholar Foundation (ts201511019). The gas adsorption-desorption studies of this research were supported as part of the Center for Gas Separations Relevant to Clean Energy Technologies, an Energy Frontier Research Center funded by the U.S. Department of Energy, Office of Science, Basic Energy Sciences under Award Number DE-SC0001015. The PXRD characterization and analysis were funded by the Robert A. Welch Foundation through a Welch Endowed Chair to HJZ (A-0030). We gratefully acknowledge Prof. Michael O'Keeffe and Mr. Gregory S. Day for the help and insightful discussion.

REFERENCES

- Zhou, H. C.; Long, J. R.; Yaghi, O. M., Introduction to Metal-Organic Frameworks. *Chem. Rev.* **2012**, *112* (2), 673-674.
- Furukawa, H.; Muller, U.; Yaghi, O. M., "Heterogeneity within Order" in Metal-Organic Frameworks. *Angew. Chem. Int. Ed.* **2015**, *54* (11), 3417-3430.

3. Cohen, S. M., Postsynthetic Methods for the Functionalization of Metal-Organic Frameworks. *Chem. Rev.* **2012**, *112* (2), 970-1000.
4. Li, J. R.; Sculley, J.; Zhou, H. C., Metal-Organic Frameworks for Separations. *Chem. Rev.* **2012**, *112* (2), 869-932.
5. Li, M.; Li, D.; O'Keeffe, M.; Yaghi, O. M., Topological Analysis of Metal-Organic Frameworks with Polytopic Linkers and/or Multiple Building Units and the Minimal Transitivity Principle. *Chem. Rev.* **2014**, *114* (2), 1343-1370.
6. Stock, N.; Biswas, S., Synthesis of Metal-Organic Frameworks (MOFs): Routes to Various MOF Topologies, Morphologies, and Composites. *Chem. Rev.* **2012**, *112* (2), 933-969.
7. Lee, J.; Farha, O. K.; Roberts, J.; Scheidt, K. A.; Nguyen, S. T.; Hupp, J. T., Metal-organic framework materials as catalysts. *Chem. Soc. Rev.* **2009**, *38* (5), 1450-1459.
8. Kirchon, A.; Feng, L.; Drake, H. F.; Joseph, E. A.; Zhou, H. C., From fundamentals to applications: a toolbox for robust and multifunctional MOF materials. *Chem. Soc. Rev.* **2018**, *47*, 8611-8638.
9. Lu, W. G.; Wei, Z. W.; Gu, Z. Y.; Liu, T. F.; Park, J.; Park, J.; Tian, J.; Zhang, M. W.; Zhang, Q.; Gentle, T.; Bosch, M.; Zhou, H. C., Tuning the structure and function of metal-organic frameworks via linker design. *Chem. Soc. Rev.* **2014**, *43* (16), 5561-5593.
10. Yuan, S.; Feng, L.; Wang, K.; Pang, J.; Bosch, M.; Lollar, C.; Sun, Y.; Qin, J.; Yang, X.; Zhang, P.; Wang, Q.; Zou, L.; Zhang, Y.; Zhang, L.; Fang, Y.; Li, J.; Zhou, H. C., Stable Metal-Organic Frameworks: Design, Synthesis, and Applications. *Adv. Mater.* **2018**, *30*, 1704303.
11. Xue, D. X.; Belmabkhout, Y.; Shekhah, O.; Jiang, H.; Adil, K.; Cairns, A. J.; Eddaoudi, M., Tunable Rare Earth fcu-MOF Platform: Access to Adsorption Kinetics Driven Gas/Vapor Separations via Pore Size Contraction. *J. Am. Chem. Soc.* **2015**, *137* (15), 5034-5040.
12. Xue, D. X.; Cairns, A. J.; Belmabkhout, Y.; Wojtas, L.; Liu, Y. L.; Alkordi, M. H.; Eddaoudi, M., Tunable Rare-Earth fcu-MOFs: A Platform for Systematic Enhancement of CO₂ Adsorption Energetics and Uptake. *J. Am. Chem. Soc.* **2013**, *135* (20), 7660-7667.
13. Guillerm, V.; Weselinski, L. J.; Belmabkhout, Y.; Cairns, A. J.; D'Elia, V.; Wojtas, L.; Adil, K.; Eddaoudi, M., Discovery and introduction of a (3,18)-connected net as an ideal blueprint for the design of metal-organic frameworks. *Nat. Chem.* **2014**, *6* (8), 673-680.
14. Bai, Y.; Dou, Y. B.; Xie, L. H.; Rutledge, W.; Li, J. R.; Zhou, H. C., Zr-based metal-organic frameworks: design, synthesis, structure, and applications. *Chem. Soc. Rev.* **2016**, *45* (8), 2327-2367.
15. Schnobrich, J. K.; Lebel, O.; Cychosz, K. A.; Dailly, A.; Wong-Foy, A. G.; Matzger, A. J., Linker-Directed Vertex Desymmetrization for the Production of Coordination Polymers with High Porosity. *J. Am. Chem. Soc.* **2010**, *132* (39), 13941-13948.
16. Yuan, S.; Chen, Y.-P.; Qin, J.-S.; Lu, W.; Zou, L.; Zhang, Q.; Wang, X.; Sun, X.; Zhou, H.-C., Linker Installation: Engineering Pore Environment with Precisely Placed Functionalities in Zirconium MOFs. *J. Am. Chem. Soc.* **2016**, *138* (28), 8912-8919.
17. Yuan, S.; Lu, W.; Chen, Y.-P.; Zhang, Q.; Liu, T.-F.; Feng, D.; Wang, X.; Qin, J.; Zhou, H.-C., Sequential Linker Installation: Precise Placement of Functional Groups in Multivariate Metal-Organic Frameworks. *J. Am. Chem. Soc.* **2015**, *137* (9), 3177-3180.
18. Cavka, J. H.; Jakobsen, S.; Olsbye, U.; Guillou, N.; Lamberti, C.; Bordiga, S.; Lillerud, K. P., A New Zirconium Inorganic Building Brick Forming Metal Organic Frameworks with Exceptional Stability. *J. Am. Chem. Soc.* **2008**, *130* (42), 13850-13851.
19. Feng, D. W.; Wang, K. C.; Su, J.; Liu, T. F.; Park, J.; Wei, Z. W.; Bosch, M.; Yakovenko, A.; Zou, X. D.; Zhou, H. C., A Highly Stable Zeotype Mesoporous Zirconium Metal-Organic Framework with Ultralarge Pores. *Angew. Chem. Int. Ed.* **2015**, *54* (1), 149-154.
20. Jiang, J. C.; Gandara, F.; Zhang, Y. B.; Na, K.; Yaghi, O. M.; Klemperer, W. G., Superacidity in Sulfated Metal-Organic Framework-808. *J. Am. Chem. Soc.* **2014**, *136* (37), 12844-12847.
21. Jiang, H.; Jia, J. T.; Shkurenko, A.; Chen, Z. J.; Adil, K.; Belmabkhout, Y.; Weselinski, L. J.; Assen, A. H.; Xue, D. X.; O'Keeffe, M.; Eddaoudi, M., Enriching the Reticular Chemistry Repertoire: Merged Nets Approach for the Rational Design of Intricate Mixed-Linker Metal-Organic Framework Platforms. *J. Am. Chem. Soc.* **2018**, *140* (28), 8858-8867.
22. Wang, B.; Lv, X. L.; Feng, D. W.; Xie, L. H.; Zhang, J.; Li, M.; Xie, Y. B.; Li, J. R.; Zhou, H. C., Highly Stable Zr(IV)-Based Metal-Organic Frameworks for the Detection and Removal of Antibiotics and Organic Explosives in Water. *J. Am. Chem. Soc.* **2016**, *138* (19), 6204-6216.
23. Wang, R. M.; Wang, Z. Y.; Xu, Y. W.; Dai, F. N.; Zhang, L. L.; Sun, D. F., Porous Zirconium Metal-Organic Framework Constructed from 2D -> 3D Interpenetration Based on a 3,6-Connected kgd Net. *Inorg. Chem.* **2014**, *53* (14), 7086-7088.
24. Lee, S.; Burgi, H. B.; Alshimri, S. A.; Yaghi, O. M., Impact of Disordered Guest-Framework Interactions on the Crystallography of Metal-Organic Frameworks. *J. Am. Chem. Soc.* **2018**, *140* (28), 8958-8964.
25. Ma, J. L.; Tran, L. D.; Matzger, A. J., Toward Topology Prediction in Zr-Based Microporous Coordination Polymers: The Role of Linker Geometry and Flexibility. *Cryst. Growth Des.* **2016**, *16* (7), 4148-4153.
26. Pang, J. D.; Yuan, S.; Qin, J. S.; Liu, C. P.; Lollar, C.; Wu, M. Y.; Yuan, D. Q.; Zhou, H. C.; Hong, M. C., Control the Structure of Zr-Tetracarboxylate Frameworks through Steric Tuning. *J. Am. Chem. Soc.* **2017**, *139* (46), 16939-16945.
27. Li, P.; Vermeulen, N. A.; Malliakas, C. D.; Gomez-Gualdrón, D. A.; Howarth, A. J.; Mehdi, B. L.; Dohnalkova, A.; Browning, N. D.; O'Keeffe, M.; Farha, O. K., Bottom-up construction of a superstructure in a porous uranium-organic crystal. *Science* **2017**, *356* (6338), 624-627.
28. Bünzli, J. C. G.; Piguet, C., Lanthanide-containing molecular and supramolecular polymetallic functional assemblies. *Chem. Rev.* **2002**, *102* (6), 1897-1928.
29. Luebke, R.; Belmabkhout, Y.; Weselinski, L. J.; Cairns, A. J.; Alkordi, M.; Norton, G.; Wojtas, L.; Adil, K.; Eddaoudi, M., Versatile rare earth hexanuclear clusters for the design and synthesis of highly-connected ftw-MOFs. *Chem. Sci.* **2015**, *6* (7), 4095-4102.
30. Luo, T. Y.; Liu, C.; Eliseeva, S. V.; Muldoon, P. F.; Petoud, S.; Rosi, N. L., Rare Earth pcu Metal-Organic Framework Platform Based on RE₄(μ₃-OH)₄(COO)₆(2⁺) Clusters: Rational Design, Directed Synthesis, and Deliberate Tuning of Excitation Wavelengths. *J. Am. Chem. Soc.* **2017**, *139* (27), 9333-9340.
31. Zhang, L. L.; Yuan, S.; Feng, L.; Guo, B. B.; Qin, J. S.; Xu, B.; Lollar, C.; Sun, D. F.; Zhou, H. C., Pore-Environment Engineering with Multiple Metal Sites in Rare-Earth Porphyrinic Metal-Organic Frameworks. *Angew. Chem. Int. Ed.* **2018**, *57* (18), 5095-5099.
32. Alezi, D.; Peedikakkal, A. M. P.; Weselinski, L. J.; Guillerm, V.; Belmabkhout, Y.; Cairns, A. J.; Chen, Z. J.; Wojtas, L.; Eddaoudi, M., Quest for Highly Connected Metal-Organic Framework Platforms: Rare-Earth Polynuclear Clusters Versatility

- 1 Meets Net Topology Needs. *J. Am. Chem. Soc.* **2015**, *137* (16),
2 5421-5430.
- 3 33. Bassett, A. P.; Magennis, S. W.; Glover, P. B.; Lewis, D. J.;
4 Spencer, N.; Parsons, S.; Williams, R. M.; De Cola, L.;
5 Pikramenou, Z., Highly luminescent, triple- and quadruple-
6 stranded, dinuclear Eu, Nd, and Sm(III) lanthanide complexes
7 based on bis-diketonate ligands. *J. Am. Chem. Soc.* **2004**, *126* (30),
8 9413-9424.
- 9 34. Chen, Z. J.; Weselinski, L. J.; Adil, K.; Belmabkhout, Y.;
10 Shkurenko, A.; Jiang, H.; Bhatt, P. M.; Guillerm, V.; Dauzon, E.;
11 Xue, D. X.; O'Keeffe, M.; Eddaoudi, M., Applying the Power of
12 Reticular Chemistry to Finding the Missing alb-MOF Platform
13 Based on the (6,12)-Coordinated Edge -Transitive Net. *J. Am.*
14 *Chem. Soc.* **2017**, *139* (8), 3265-3274.
- 15 35. Blatov, V. A. T. P., Commission on Crystallographic
16 Computing, IUCr, 2006.
- 17 36. Yuan, S.; Chen, Y. P.; Qin, J. S.; Lu, W. G.; Wang, X.; Zhang,
18 Q.; Bosch, M.; Liu, T. F.; Lian, X. Z.; Zhou, H. C., Cooperative
19 Cluster Metalation and Ligand Migration in Zirconium Metal-
20 Organic Frameworks. *Angew. Chem. Int. Ed.* **2015**, *54* (49), 14696-
21 14700.
- 22 37. Dong, Z. Y.; Sun, Y. Z. S.; Chu, J.; Zhang, X. Z.; Deng, H. X.,
23 Multivariate Metal-Organic Frameworks for Dialing-in the
24 Binding and Programming the Release of Drug Molecules. *J. Am.*
25 *Chem. Soc.* **2017**, *139* (40), 14209-14216.
- 26 38. Yang, J. J.; Zhang, Y. B.; Liu, Q.; Trickett, C. A.; Gutierrez-
27 Puebla, E.; Monge, M. A.; Cong, H. J.; Aldossary, A.; Deng, H. X.;
28 Yaghi, O. M., Principles of Designing Extra-Large Pore Openings
29 and Cages in Zeolitic Imidazolate Frameworks. *J. Am. Chem. Soc.*
30 **2017**, *139* (18), 6448-6455.

Table of Contents

